

MECHANICAL PROPERTIES AND MICROSTRUCTURAL EVOLUTIONS AT HIGH STRAIN RATES OF ELECTRODEPOSITED NICKEL

H. Couque¹, A. Ouarem², G. Dirras² and J. Gubicza³

Summary – The mechanical and microstructural characteristics of high purity nickel processed by electrodeposition tested in compression up to a dynamic strain rate of $1.5 \times 10^5 \text{ s}^{-1}$ using a direct impact Hopkinson pressure bar technique have been analyzed. The nickel exhibits thermal activated strain rate sensitivity up to about 10^3 s^{-1} . At higher rates, a sharp increase of the strength is observed related to dislocation drag effects known as the viscous regime. This strain rate dependence is best reproduced through a modified Johnson-Cook constitutive model uncoupling the strain rate dependence and the temperature dependence. Microstructure analyses reveal an increase of the average grain size with the strain rate increasing up to about $1 \times 10^4 \text{ s}^{-1}$ and are related to the reduction of amount of twins. The twin structure generated in the early shock stage of the loading evolves through dislocation interactions during the plastic deformation occurring under unshocked conditions. At a higher strain rate of $1.5 \times 10^5 \text{ s}^{-1}$, the grain size is decreasing to the value similar to initial state. At this strain rate, high dislocation density along with the temperature increase due to plastic deformation might favour dynamic recrystallization thus resulting in a decrease of the grain size.

Keywords – nickel, recrystallization, high strain rate

First TMS-ABM International Materials Congress "Dynamic Behavior of Materials", July 26-30, 2010, Rio de Janeiro, Brazil

¹ Nexter Munitions, 7 route de Guerry, 18023 Bourges, France

² Laboratoire des Propriétés Mécaniques et Thermodynamiques des Matériaux, UPR CNRS 9001, 99 avenue J.B. Clément, 93430 Villetaneuse, France

³ Department of Materials Physics, Eötvös Lorand University, P.O.B. 32, H-1518, Budapest, Hungary

INTRODUCTION

Structural materials like nickel (Ni) are employed in military applications such as liner of explosively formed projectiles [1]. During the phase formation of the projectile, the liner material experiences large deformation under high strain rate, that could modify the as-processed microstructure by means of thermomechanical processes mostly due to the increase of temperature. Particularly dynamic recrystallization was reported to occur during extreme deformations [2,3].

The present study reports about high purity electrolytic Ni samples containing a large fraction of $\Sigma 3$ coherent twin boundaries in the as-processed state tested at strain rates ranging from 2.3×10^3 to $2.2 \times 10^5 \text{ s}^{-1}$ with a direct impact Hopkinson pressure bar system [4]. The experimental data previously reported by Couque et al. [1] have been revisited to precise strain rate and strain histories. The evolution of the microstructure from the thermal activated strain rate regime to the viscous regime and its influence on the subsequent mechanical behavior are investigated.

EXPERIMENTAL APPROACHES

The chemical composition of the high purity (99.99 %) electrolytic Ni material is given in Table 1.

From the as-received square plates, cylinders of 9.0 mm in diameter and 5.0 mm in height were prepared and subsequently dynamically deformed in compression using a direct impact Hopkinson pressure bar test (DHPB) at strain rate ranging from 2.4×10^3 to $1.5 \times 10^5 \text{ s}^{-1}$.

Table 1. Chemical composition (in percent) of the as-received Ni material.

Ni	Co	Cu	Zn	Fe	P	C	S	Pb
Balance	0.0003	0.0010	0.0005	0.0030	0.0002	0.0050	0.0005	0.0001

The DHPB technique, originally introduced by Dharan [5], consists in impacting at a constant velocity with a striker a specimen placed against a Hopkinson pressure bar, as shown in Figure 1. The striker speed, V_i , typically between 5 and 100 m s^{-1} , is recorded using two lasers beams separated by 18 mm and positioned 30 mm prior impact. Tests were conducted at three impact velocities of 10.9, 28.2 and 70.6 m s^{-1} . Both striker and Hopkinson bar are made of tungsten alloy bars, whose characteristics are: 20 mm in diameter, 17.5 g cm^{-3} in density and 1500 MPa in yield stress.

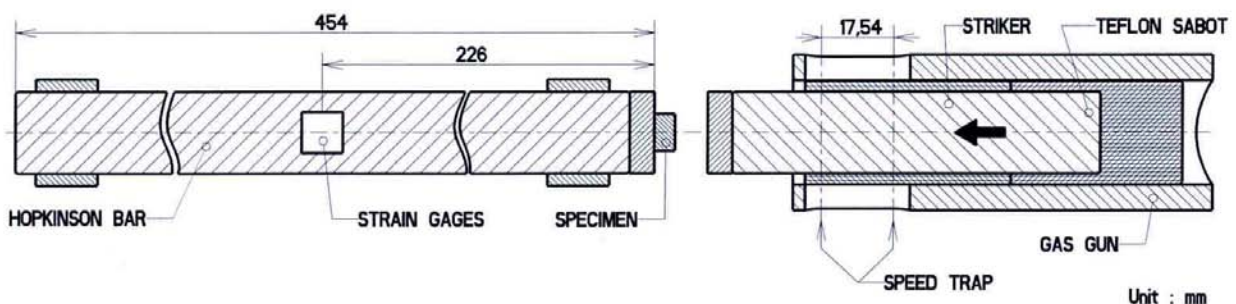


Figure 1. Direct impact Hopkinson pressure bar technique (DHPB).

The true deformation is obtained from the specimen end displacements with the specimen / bar interface deduced from the strain history, $\varepsilon_T(t)$, of the Hopkinson bar using strain gages, and with the specimen / striker interface displacement rate equal to V_i :

$$\varepsilon(t) = \text{Ln} (1 + \varepsilon_n(t)) = \text{Ln} (1 + (V_i t - C_o \int_0^t \varepsilon_T(\tau) d\tau) / H_o)) \quad (1)$$

where H_o is the specimen height, and C_o is the sound velocity of the Hopkinson bar material. With the assumption that plastic deformation is isochoric, the specimen axial stress is obtained from the strain history, $\varepsilon_T(t)$, of the Hopkinson bar:

$$\sigma_x(t) = \sigma_n(t) (1 + \varepsilon_n(t)) = \rho C_o^2 \varepsilon_T(t) S_T/S_o (1 + \varepsilon_n(t)) \quad (2)$$

where ρ is the density of the Hopkinson bar, S_T and S_o are the section area of the Hopkinson bar and specimen, respectively. Due to inertia, the radial and tangential stresses, $\sigma_r(t)$ and $\sigma_\theta(t)$, are:

$$\sigma_r(t) = \sigma_\theta(t) = (3/8) \rho (R_o V_i / H_o)^2 (1 - \varepsilon_n(t))^{-3} \quad (3)$$

The equivalent stress is then derived:

$$\sigma(t) = \sigma_x(t) - \sigma_r(t) = \rho C_o^2 \varepsilon_T(t) S_T/S_o (1 + \varepsilon_n(t)) - (3/8) \rho (R_o V_i / H_o)^2 (1 - \varepsilon_n(t))^{-3} \quad (4)$$

Microstructure investigations of the as received, impacted specimens were carried out mainly by scanning electron microscopy (SEM) and electron backscattering diffraction (EBSD) technique. The EBSD investigations were conducted over regions of approximately 150 μm x 150 μm using a step size between neighbouring measurement positions of 0.1 μm . The average grain size, the fraction of high angle grain boundaries (HAGBs) and especially $\Sigma 3$ coherent twin boundaries were extracted from the EBSD analyses. Finally, the influence of microstructure evolution on the quasi-static mechanical behavior was investigated by nanohardness measurements carried out on both the initial and impacted samples using a UMIS nanoindentation device with Berkovich indenter and applying a maximum load of 5 mN. The indentation rate was 0.15 m N s⁻¹ [4].

RESULTS AND DISCUSSION

The high strain rate data are provided in Table 2 and Figure 2. The strain responses have been corrected by subtracting the linear part of the response corresponding to the elastic loading phase, see Figure 2. The final axial strains provided in Table 2, ε_f , were approximated using the true strain - engineering strain relation, $\varepsilon_f = \text{Ln} (1+e)$, with e the engineering strain. The strain rate in Figure 2 and Table 2 has been calculated from the derivative of Eqn. (1). For strain greater than 0.5 where a uniaxial state of stress does not prevail anymore, the derivative of Eqn. (1) provides an overestimation of the strain rate by about 10%. With regard to the test conducted at 10.9 m s⁻¹, the mass of the striker was insufficient to provide a constant impact velocity during the entire plastic deformation, resulting in a final strain using Eqn. (1) of 0.18 overestimating by 28% the measured final strain of 0.14.

Table 2. Sample characteristics with D_o , H_o , and D_f , H_f , the specimen diameter and height before impact, and after impact at a velocity V_i , respectively. The engineering strain, e , an estimate of the true strain, ϵ_f , the initial and final plastic strain rate, $\dot{\epsilon}_i$ and $\dot{\epsilon}_f$, respectively are also reported.

V_i (m s ⁻¹)	D_o (mm)	H_o (mm)	D_f (mm)	H_f (mm)	e	ϵ_f	$\dot{\epsilon}_i$ (s ⁻¹)	$\dot{\epsilon}_f$ (s ⁻¹)
10.9	9.01	5.01	9.86	4.34	-0.132	-0.14	-2400	-2900
28.2	9.01	5.00	12.89	2.48	-0.504	-0.70	-5900	-12500*
70.6	9.01	5.02	19.50	0.53	-0.894	-2.24	-14500	-156000*

*estimated

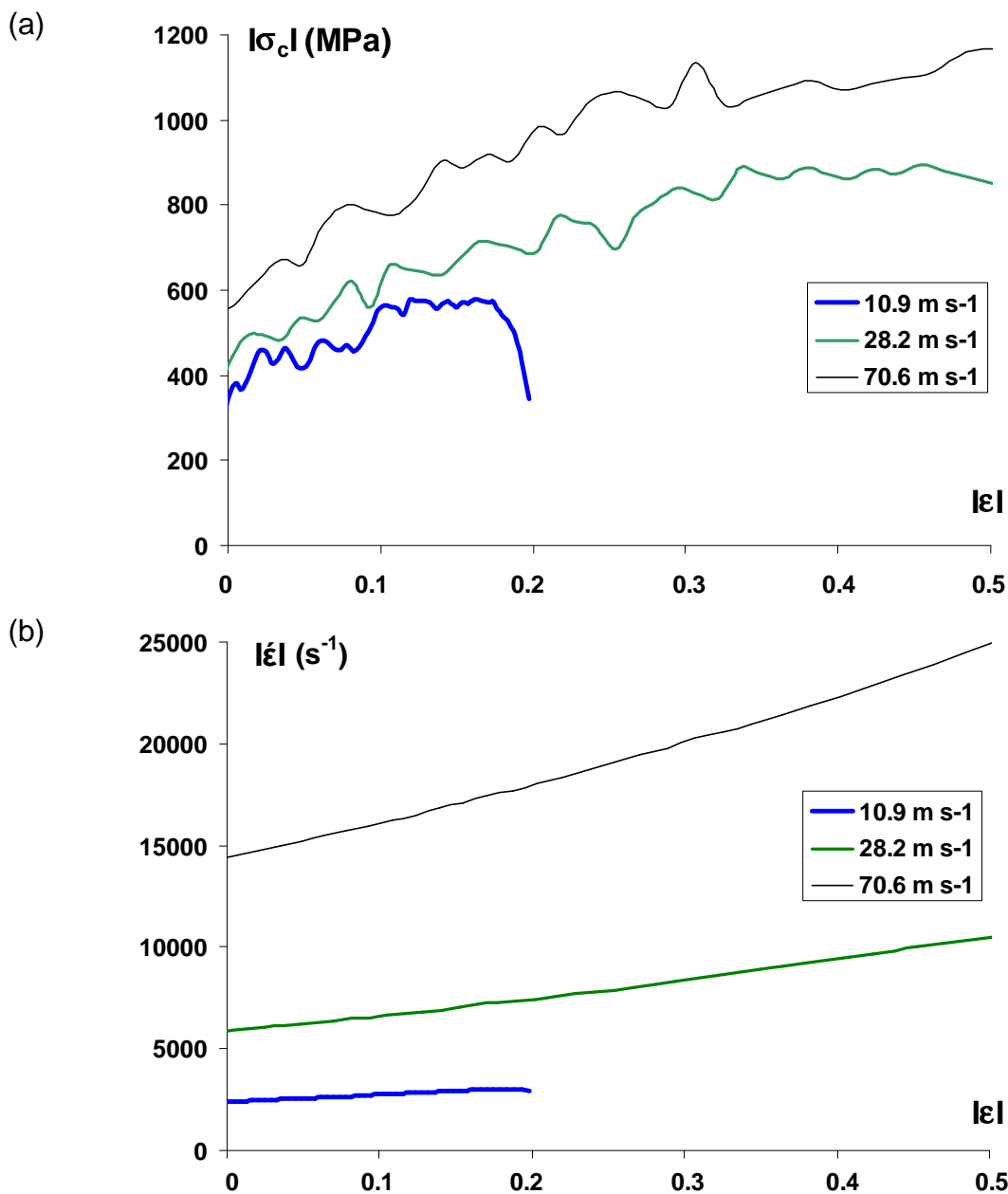


Figure 2. Stress strain (a) and strain-rate strain (b) responses of the Ni specimens tested at 10.9, 28.2 and 70.6 m s⁻¹ with the DHPB technique.

Figure 3a plots the stress at a plastic strain of 0.05 versus strain rate revealing the thermally activated regime and the viscous regime [6] associated to the dislocation drag effects occurring in the present case at about 10^3 s^{-1} . As it can be seen in Figure 3, the classical Johnson-Cook constitutive model [7] does not describe the strengthening occurring in the viscous regime. As reported by Couque et al. [1], the Zerilli-Amstrong constitutive model [8] and a modified Johnson-Cook constitutive model were found to reproduce the sharp turn of the strength observed in the 10^3 - 10^4 s^{-1} transition regime. However, because the strain rate and temperature terms of the Zerilli-Amstrong model are coupled, the elevated temperature data cannot be reproduced. In the contrary, a good agreement was reached at both extremes, temperature and strain rate, for the modified Johnson-Cook model.

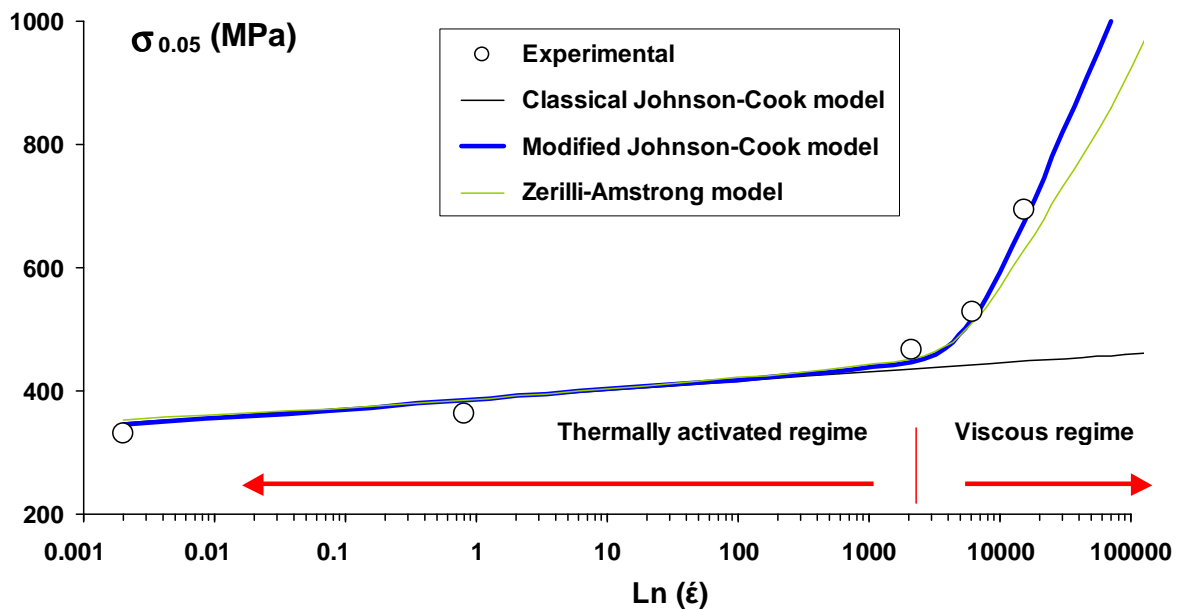


Figure 3. Stress strain-rate dependence of the nickel at a plastic strain of 0.05.

The modified Johnson-Cook model includes a power strain rate component added to the logarithm strain rate term of the original Johnson-Cook formulation, $D(\dot{\epsilon} / \dot{\epsilon}_1)^k$, with D and k two constants. This component is normalized by a reference strain rate, $\dot{\epsilon}_1$, characterizing the transition between the thermally activated regime and the viscous regime, which is about 10^3 s^{-1} . The equivalent stress function of plastic strain, ϵ_p , strain rate, $\dot{\epsilon}$, and temperature, T , is expressed as:

$$\sigma = (A + B \epsilon_p^n) (1 + C \ln(\dot{\epsilon} / \dot{\epsilon}_0) + D(\dot{\epsilon} / \dot{\epsilon}_1)^k) (1 - [(T - T_r) / (T_m - T_r)]^m), \quad (5)$$

with T_r and T_m are the room and melting temperatures, respectively, $\dot{\epsilon}_0$, the reference strain rate equal to 1 and A , B , C , n , m the five constants of the original Johnson-Cook model. This formulation enables to go back to the classical formulation when strain rates are lower than 10^3 s^{-1} .

Microstructure investigations revealed that the microstructure of the initial state is composed of equiaxed grains (Fig. 4a). The majority of grain boundaries, about 97%, are HAGBs (with misorientation across the boundary larger than 15°) including $\Sigma 3$ boundaries (with misorientation of about 60°), whose fraction is about 50%. The average grain size determined from the areas bounded by HAGBs in the EBSD images was about 3.9 μm . For the sample impacted at velocities of 10.9 and 28.2 m s^{-1} , the HAGBs fraction sharply decreased to 38% and 57% and that of $\Sigma 3$ boundaries from about 38% to 7%, respectively [4]. The average grain size determined from the area of grains bounded by HAGBs increased from 4.5 μm to 6 μm , respectively, and appears to be associated to the decrease of the $\Sigma 3$ boundaries.

The most striking effect was that the microstructure of the sample impacted at the highest velocity of 70.6 m s^{-1} , was qualitatively similar to that of the initial state (Fig. 4b) in terms of both HAGBs fraction and grain size, yielding 92% and about 3.7 μm , respectively. Nevertheless, visual observation indicates that the fraction of TBs within the $\Sigma 3$ boundaries is drastically reduced compared with the initial state. It is likely that dynamic recovery/recrystallization occurred here and led to a microstructure close to that of the initial. It should be noticed that dynamic recrystallization during high strain rate deformation has been also reported in previous works [2,3].

The recrystallization process of the specimen tested at 70.6 m s^{-1} apparently comes from the heat conversion of the large plastic deformation occurring under adiabatic conditions. Assuming 90% of the plastic work W_p was converted (Taylor-Quinney coefficient equal to 0.9), the temperature increase is given by $\Delta T = 0.9W_p / (\rho C_p)$, where ρ is the mass density and C_p is the specific heat at constant pressure. The ρ and C_p values for Ni are 8908 kg m^{-3} and 446 $\text{J kg}^{-1} \text{K}^{-1}$, respectively. The temperature increase due to plastic work is about 646 K implying a homologous temperature $T/T_m = 0.55$, where T is the temperature after the impact and T_m is the melting temperature of Ni (1728 K). This ratio is above, $T/T_m = 0.40$, the onset when diffusional processes become important to trigger dynamic recrystallization [2].

Dirras et al. [4] have performed line profile analyses investigations in the non-recrystallized volumes of the sample tested at 70.6 m s^{-1} which revealed an increase of the twin probability. The authors attributed this increase to the viscous dislocation drag effect becoming preponderant when strain rates exceed $1.5 \times 10^4 \text{ s}^{-1}$. This is, because the local stresses might reach the critical stress required for twin nucleation. This result goes along with data generated at very high strain rates under shock, where a transition occurred from plasticity controlled by dislocation or twinning defect movements to control by slip or twinning defect generations [9].

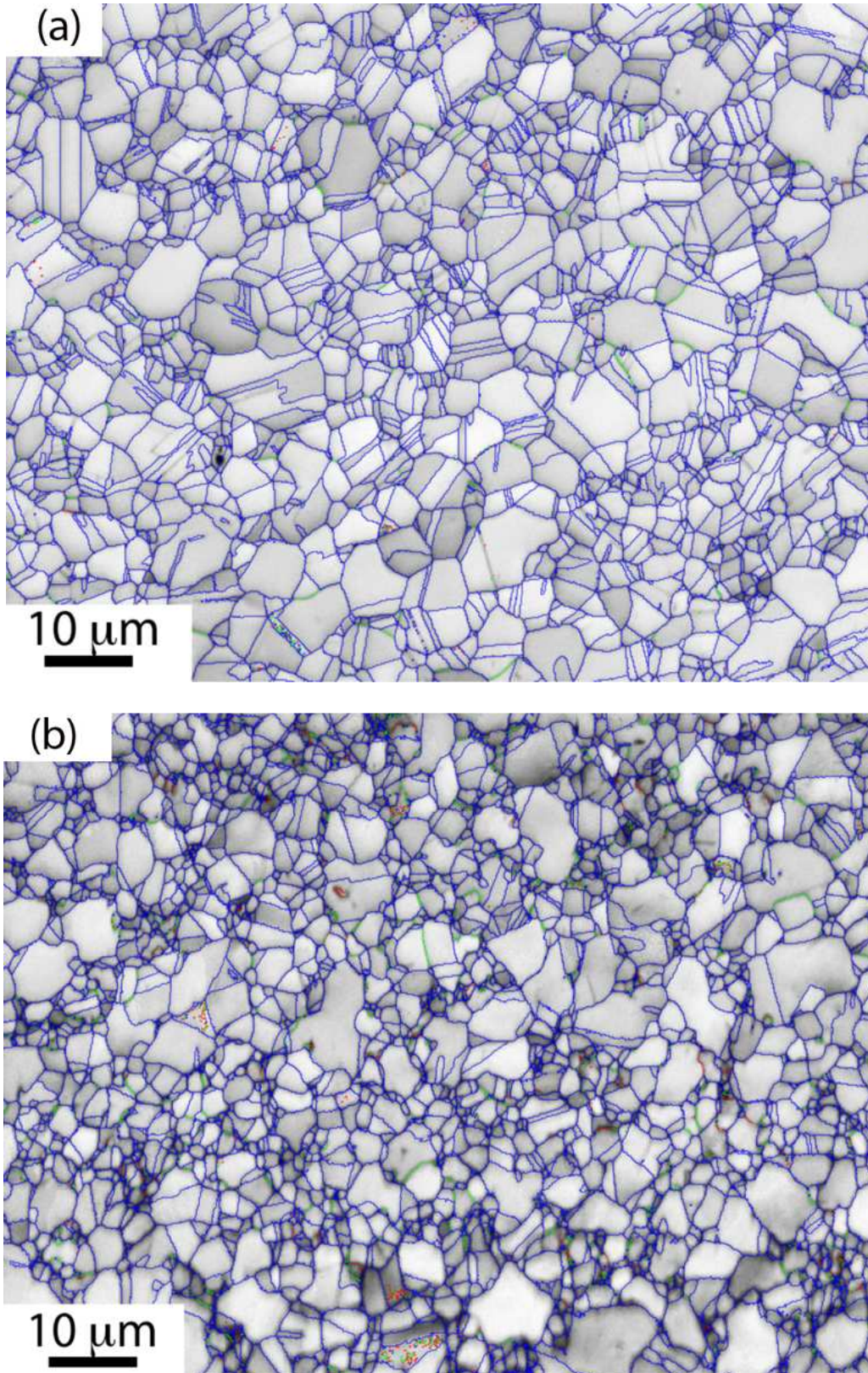


Figure 4. EBSD images illustrated the evolution of the $\Sigma 3$ coherent twin boundaries of investigated Ni samples, (a) initial state; (b) after direct impact at 70.6 m s^{-1} .

Nanoindentation tests were carried out to make sure of the occurrence of recovery/recrystallization during impact test at the highest velocity [4]. Table 3 provides the mean nanohardness average for the initial state and for the impacted samples. The increase of the mean nanohardness with the increase of the impact velocity from 10.9 to 28.2 m s⁻¹ can be attributed to an increase of the dislocation density. After the impact test at 70.6 m s⁻¹ the mean nanohardness decreased to the same value as in the initial case. This can be explained only by the occurrence of recovery/recrystallization.

Table 3. Mean nanohardness of the initial specimen and for the impacted samples.

	Initial state	$V_i = 10.9 \text{ m s}^{-1}$	$V_i = 28.2 \text{ m s}^{-1}$	$V_i = 70.6 \text{ m s}^{-1}$
Hardness (GPa)	2.7	3.1	5.1	2.7

CONCLUSIONS

High purity nickel samples deformed dynamically in compression using a direct impact Hopkinson pressure bar technique (DHPB) at impact velocities of 10.9, 28.2 and 70.6 m s⁻¹ were found to cover strain rates ranging from 2.4×10^3 to $1.5 \times 10^5 \text{ s}^{-1}$. When considering quasi-static data, the stress increases linearly as a function of the logarithm of the strain rate up to 10^3 s^{-1} corresponding to the thermally activated regime. A strong increase of the stress, with a power dependence of the strain rate, is then observed known as the viscous regime associated to the drag dislocation effects. These regimes can be described through the uncoupling of the strain rate dependence and temperature dependence, using a modified Johnson Cook constitutive model [1]. The model expresses the stress with a strain rate function dissociating the thermally activated regime through logarithm strain-rate dependence, and the viscous regime through power strain-rate dependence.

A microstructure characterization revealed that up to a velocity of 28.2 m s⁻¹, the dislocation density in the impacted samples increased which was accompanied by the reduction of the fraction of $\Sigma 3$ type boundaries. The increase of the dislocation density yielded an increase of both nanohardness. The decrease of the amount of $\Sigma 3$ type boundaries, that initially divide grains into smaller areas, caused an apparent increase of the mean grain size measured by EBSD.

At the higher impact velocity, 70.6 m s⁻¹, it was observed that the microstructure resembled to that of the initial. The nanohardness was also the same as in the initial state. These features are typical of dynamic recovery/recrystallization processes taking place during the impact test most probably due to the increase of the homologous temperature to about 0.55.

Further investigations are being conducted to compare microstructural features at a fixed axial strain of 0.2. Such investigations will permit to confirm that the viscous dislocation drag effect plays a major role in the increase of the twin probability observed at strain rates above $1.5 \times 10^4 \text{ s}^{-1}$ in the non-recrystallized zones of the sample tested at 70.6 m s⁻¹. These data may support the uncoupled strain rate and temperature dependences, suggested by the modified Johnson Cook constitutive model.

Acknowledgements

The authors express their thanks to MM. P. Vanneau and Y. Menard for conducting the compression tests.

REFERENCES

- [1] H. Couque and R. Boulanger, in: F. Gálves, V. Sanchez-Galves (Eds.), 23rd Int. symposium on Ballistics (2007) 255-262.
- [2] M. A. Meyers, V. F. Nesterenko, J. C. La Salvia, Y. B. Xu and Q; Xue, DYMAT 2000 cf., *J. Phys. IV*, 9 (2000) 51-56.
- [3] L. E. Murr and C. Pizana, *Metall. Mater. Trans. A*, 38A (2007) 2611-2628.
- [4] G. Dirras, H. Couque, J. Gubicza, A. Ouarem, T. Chauveau and P. Jenei, *Mat. Sc. Eng. A.*, [doi:10.1016/j.msea.2010.03.045](https://doi.org/10.1016/j.msea.2010.03.045)
- [5] C. K. H. Dharan and F. E. Hauser, *Exp. Mech.*, 10 (1970) 370-376.
- [6] P. S. Follansbee, G. Regazzoni and U. F. Kocks, Mechanical properties at High Rates of Strain cf., *Inst. Phys. Conf. Ser.*, 70 (1984) 71-77.
- [7] G. R. Johnson and W. H. Cook, high strain rates and high temperatures, 7th *International Symposium on Ballistics* (1983) 541-548.
- [8] R. W. Armstrong and F. J. Zerilli, DYMAT 1988 cf., *J. Phys. IV*, 49, (1988) 529-534.
- [9] R. W. Armstrong and S. M. Walley, *Int. Mater. Rev.* 53 (2008) 105-128.

MECHANICAL PROPERTIES AND MICROSTRUCTURAL EVOLUTIONS AT HIGH STRAIN RATES OF ELECTRODEPOSITED NICKEL

H. Couque¹, A. Ouarem², G. Dirras² and J. Gubicza³

Summary – The mechanical and microstructural characteristics of high purity nickel processed by electrodeposition tested in compression up to a dynamic strain rate of $1.5 \times 10^5 \text{ s}^{-1}$ using a direct impact Hopkinson pressure bar technique have been analyzed. The nickel exhibits thermal activated strain rate sensitivity up to about 10^3 s^{-1} . At higher rates, a sharp increase of the strength is observed related to dislocation drag effects known as the viscous regime. This strain rate dependence is best reproduced through a modified Johnson-Cook constitutive model uncoupling the strain rate dependence and the temperature dependence. Microstructure analyses reveal an increase of the average grain size with the strain rate increasing up to about $1 \times 10^4 \text{ s}^{-1}$ and are related to the reduction of amount of twins. The twin structure generated in the early shock stage of the loading evolves through dislocation interactions during the plastic deformation occurring under unshocked conditions. At a higher strain rate of $1.5 \times 10^5 \text{ s}^{-1}$, the grain size is decreasing to the value similar to initial state. At this strain rate, high dislocation density along with the temperature increase due to plastic deformation might favour dynamic recrystallization thus resulting in a decrease of the grain size.

Keywords – nickel, recrystallization, high strain rate

First TMS-ABM International Materials Congress "Dynamic Behavior of Materials", July 26-30, 2010, Rio de Janeiro, Brazil

¹ **Nexter Munitions, 7 route de Guerry, 18023 Bourges, France**

² **Laboratoire des Propriétés Mécaniques et Thermodynamiques des Matériaux, UPR CNRS 9001, 99 avenue J.B. Clément, 93430 Villetaneuse, France**

³ **Department of Materials Physics, Eötvös Lorand University, P.O.B. 32, H-1518, Budapest, Hungary**